Effects of Bombarding Ions on the Void Swelling Profile in Nickel

J.B. Whitley, G.L. Kulcinski, H.V. Smith, Jr., and P. Wilkes

July 1978

UWFDM-252

ASTM-STP-683, 125 (1979).

FUSION TECHNOLOGY INSTITUTE

UNIVERSITY OF WISCONSIN

MADISON WISCONSIN

Effects of Bombarding Ions on the Void Swelling Profile in Nickel

J.B. Whitley, G.L. Kulcinski, H.V. Smith, Jr., and P. Wilkes

Fusion Technology Institute
University of Wisconsin
1500 Engineering Drive
Madison, WI 53706

http://fti.neep.wisc.edu

July 1978

UWFDM-252

ASTM-STP-683, 125 (1979).

Effects of Bombarding Ions on the Void Swelling Profile in Nickel

J. B. Whitley
G. L. Kulcinski
H. V. Smith, Jr.
P. Wilkes

UWFDM-252

July 1978

Presented at the Ninth International Symposium on the Effects of Radiation on Structural Materials, Richland, Washington, July 1978. Sponsored by ASTM.

Effects of Bombarding Ions on the Void Swelling Profile in Nickel

J.B. Whitley, G.L. Kulcinski, H.V. Smith, Jr., and P. Wilkes

Specimens of high purity nickel were irradiated with high energy carbon and aluminum ions to study the effect on the void microstructure of using different bombarding species. The depth dependent damage structure was determined by preparing the foils such that they could be viewed directly in cross section. These results were then compared to previous irradiations performed on identical material using self-ions. The swelling behavior observed in the end-of-range region for all samples was similar, implying that impurities introduced by the ion beam do not strongly influence the swelling response of the material. The mass of the irradiating ions had no noticeable effect on the swelling values achieved for similar damage states, even though the recoil energy spectrum produced by the various ions were different. Under aluminum ion irradiation, the void density passed through a maximum at a dose < 2 dpa and then decreased continuously with increasing dose. Voids were also observed in all specimens at depths ≈15% beyond the predicted end-of-range.

I. Introduction

The increased use of heavy-ion beams as a tool for studying irradiation induced void formation in metals has led to an interest in examining the depth dependence of the damage structure. The character of the heavy-ion damage mechanism changes considerably as the ion loses energy and by examining the depth dependence of the final damage state, one can gain an understanding of the irradiation damage process. The various techniques that have been used to determine the depth dependent structure include successive thinning of transmission electron microscope (TEM) samples,[1] stereoviewing in a high-voltage electron microscope,[2-4] and preparation of TEM specimens for viewing directly in cross section.[5-9] Of these techniques, the latter is the most direct and powerful, but it is only easily applied to metals that can be electroplated with coatings of similar chemical composition.

The authors have previously used the cross sectioning technique to study the depth dependent microstructure of high purity nickel irradiated with 14 MeV nickel and 14-19 MeV copper ions.[5,6,10] In these studies, voids were found at depths ≈20% beyond the maximum ion range predicted by various stopping theories,[11,12] and the void swelling profile was not simply related to the total damage profile. No major differences in microstructure were observed between the nickel and copper ion irradiated samples.

This paper presents the depth dependent microstructure development in high purity nickel irradiated at 525°C with carbon ions or with aluminum ions. These results will be compared with previous results obtained from self-ion irradiations. The comparative results of these irradiations will be analyzed in terms of the differences in the damage processes by ions of

different masses and different chemical species. Specifically, comparisons will be made to other irradiation studies of nickel containing small additions of carbon or aluminum before irradiation.[13,14]

II. Experimental Procedure

Details of the irradiation facility and sample target chamber[15,16] and the post-irradiation specimen techniques[5,6] can be found elsewhere. In brief, the specimens consisted of 0.5 mm thick nickel foil with nominal purity >99.995%. The ions used for this study were produced by an ANIS[17] negative ion source and accelerated in a tandem Van De Graaff accelerator to produce 5 MeV C, 8.1 MeV Al, and 14 MeV Ni ions. The damage curves calculated by the Brice code[11]* are shown for these three ions in figure 1. The ion energies were chosen such that the ions would have similar ranges in the target. The gross damage effectiveness as measured in displacements per atom (dpa) however, is quite different for the three ions as can be seen by the different scales for the various ions. Note that within each specimen, there exists both a large variation in the final damage level and also a corresponding variation in the displacement rate at which this level was achieved. The specimens were annealed at 850°C for one hour in an inert gas atmosphere and electropolished prior to loading into the target chamber. The specimens were irradiated in an ultra-high vacuum, high temperature sample chamber with a nominal pressure of 1×10^{-8} torr (1.3×10^{-6} Pa). After irradiation the specimens were prepared in cross sections by electroplating a 1 to 1.5 mm thick nickel deposit onto both sides and then slicing in a plane normal to the original foil surface using a low speed diamond saw. Three

*The conversion to displacements assumed a displacement energy of 40 eV and used the recommended practice for neutron damage simulation by charged particle irradiation, E 521-76 (Prepared under ASTM Committee E-10, Subcommittee E 10.08, 1974).

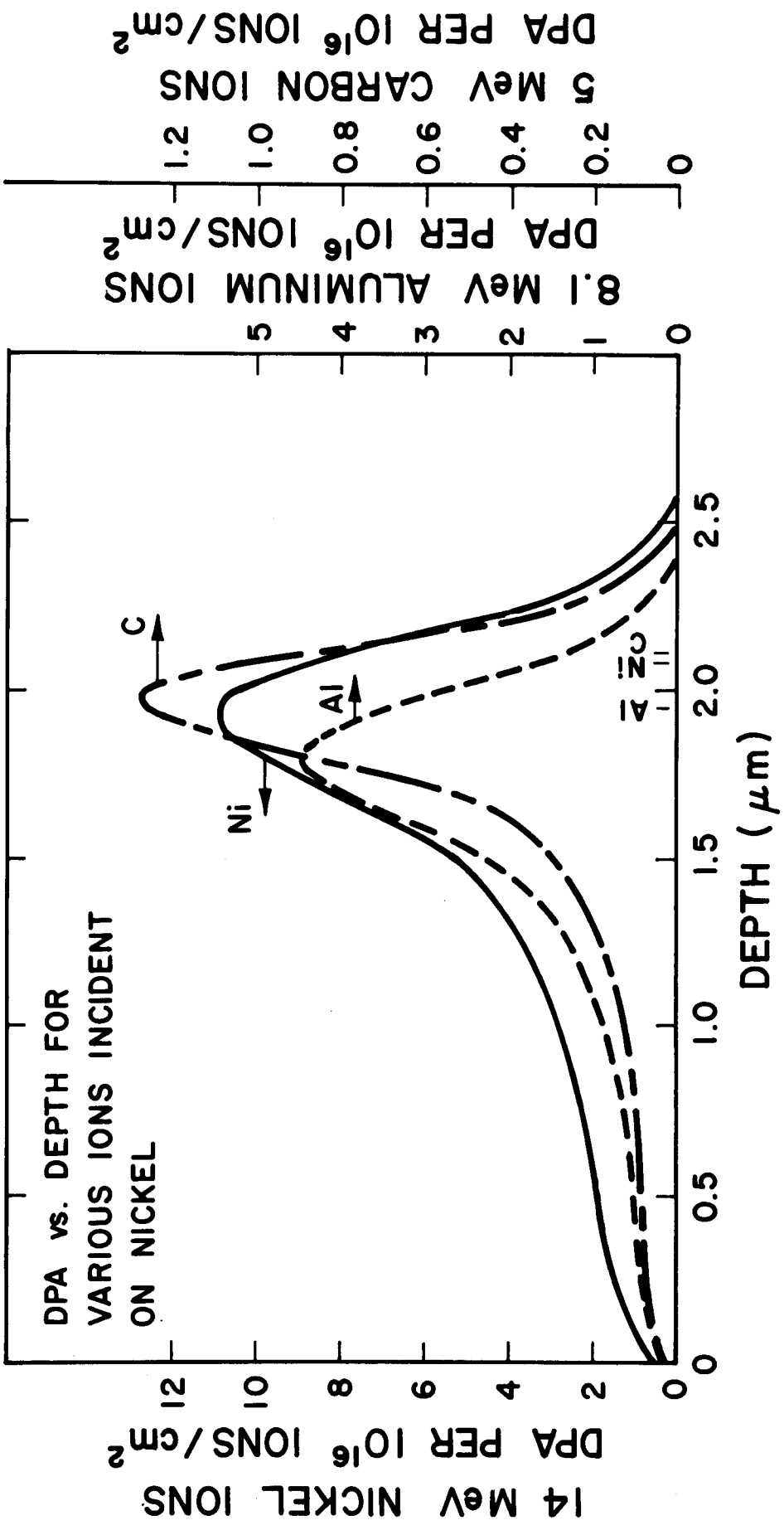

Figure 1. The calculated displacement curves for carbon, aluminum, and nickel ions incident on a nickel target. The stopping parameters were calculated using the Brice code.[11] (See footnote 1) Note the different scale values of each curve. Also shown near the base of the curves are the mean ion ranges given by the code.

millimeter discs were then removed and the samples polished in a conventional twin jet electro-polishing unit and examined in a 120 kV electron microscope.

III. Results

A. Aluminum Ion Irradiations

Nickel samples were irradiated at 525°C (798°K) with 8.1 MeV aluminum ions with fluences ranging from 4×10^{15} ions/cm^2 to 2.1×10^{16} ions/cm^2. The ion flux used was typically 8×10^{11} ions/cm^{2}s ($\approx 4 \times 10^{-4}$ dpa/s at the peak). The development of the depth dependent microstructure is shown in the micrographs of figure 2. The left-hand-side of each micrograph shows the original foil surface. The incident ions have traveled from left to right and came to rest in the area near the right-hand-side of each micrograph. Voids nucleated quite readily in this material and were observed at all damage levels. The voids were always observed in these samples up to depths of 2.75 μm, with a few voids observed at even greater depths. There was no deviation in the void microstructure in the implanted range region that could be attributed to point defect interaction with aluminum ions. The voids were truncated octahedra throughout the damage region.

Void data was obtained from these specimens by dividing each into depth intervals 0.25 μm wide parallel to the foil surface. Average void diameter, void density, and void volume fraction where then measured within each interval. Foil thickness was determined by tilting the foil and measuring the parallax of contamination markers placed on the foil surfaces. Figure 3 shows these data obtained for two fluence levels. The data points for each interval are plotted as points and not as histograms, with the curves drawn to aid the eye in following the depth variation in void parameters. At low fluences (figure 3a) the void density curve has the same general shape as the displacement curve. At high fluences, however, the void density has dropped significantly and shows much less variation in magnitude from the front surface to the end-of-range than at low

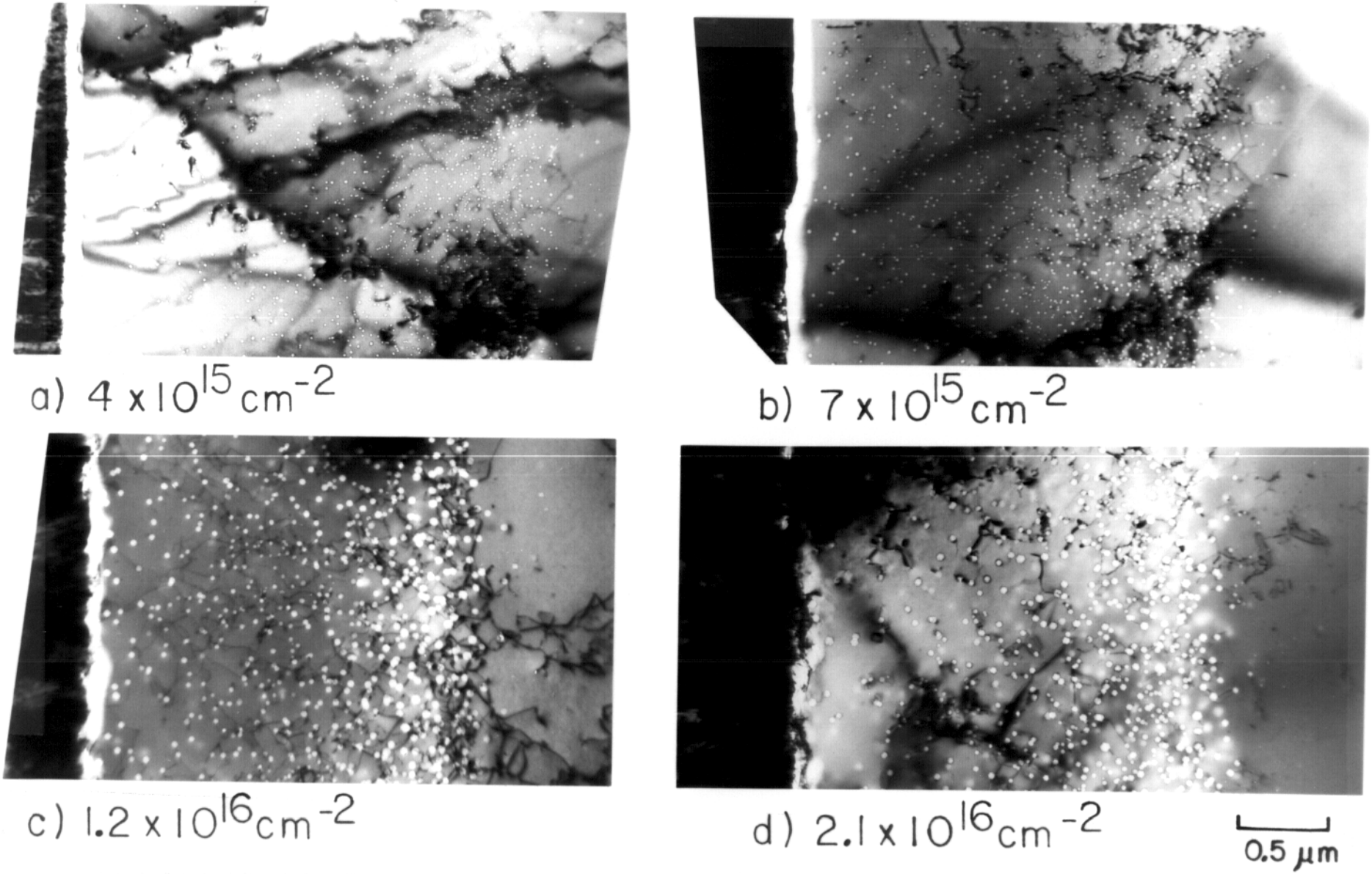

Figure 2. Nickel irradiated at 525°C (798°K) with 8.1 MeV aluminum ions to four fluence levels. The original foil surface is visible near the left-hand-side of each micrograph. The aluminum ions came to rest near the right-hand-side.

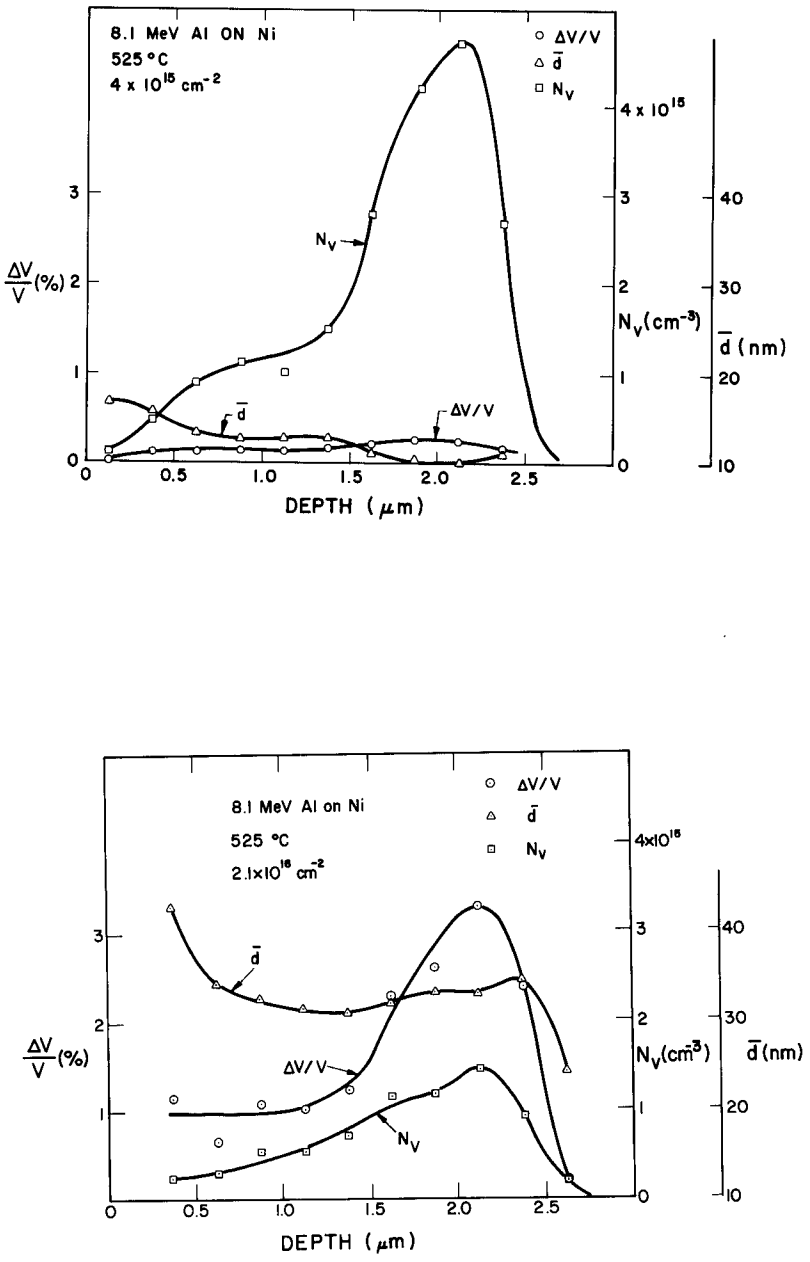

Figure 3. Average void diameter $\bar{d}$, void density N_V, and void volume fraction $\Delta V/V$ measured as a function of depth in nickel irradiated with aluminum ions. a) after a fluence of 4×10^{15} ions/cm^2; b) after a fluence of 2.1×10^{16} ions/cm^2. The curves serve only to guide the eye.

fluences. Except for the near surface region where larger voids are observed, the average void size throughout the damage region does not vary significantly. The void size distribution as a function of dose at two different depths is shown by the histograms of figure 4. The width of the void size distribution is narrower in the midrange region than in the end-of-range region, even though the average void sizes in the high dose case are not significantly different. The region of peak void swelling occurs at about 2.1 μm reaching a value of 3.3%. The theoretical peak damage level in this sample occurred at 1.8 μm reaching a value of 9.5 dpa.

B. Carbon Ion Irradiation

The carbon ion irradiations were carried out on specimens prepared identically to those for the aluminum irradiation and the irradiation was conducted at 525°C (798°K). The carbon ion flux was 4×10^{12} ions/cm^2·s (5×10^{-4} dpa/s at the peak) and the ion fluences were 1.5×10^{16} ions/cm^2 and 9.3×10^{16} ions/cm^2. The void structures developed from these irradiations are shown in figure 5, where again the original foil surface is shown on the left-hand-side of the micrographs. Voids were once more observed throughout the entire damage region (even down to 0.2 dpa), indicating the ease with which voids could nucleate in these samples. Most voids were observed in these samples at depths less than 2.85 μm, with a few voids seen at depths up to 3.2 μm. There is a slight increase in the void size at the end-of-range. Void shapes were again truncated octahedra.

The plots of void density, void size and void volume fraction for the two carbon ion fluences are shown in figure 6. The void density curve is noticeably broader than the displacement curve in this case. The void density does not drop as rapidly with dose as in the aluminum ion irradiation, nor does the void size vary strongly with depth except for the surface region

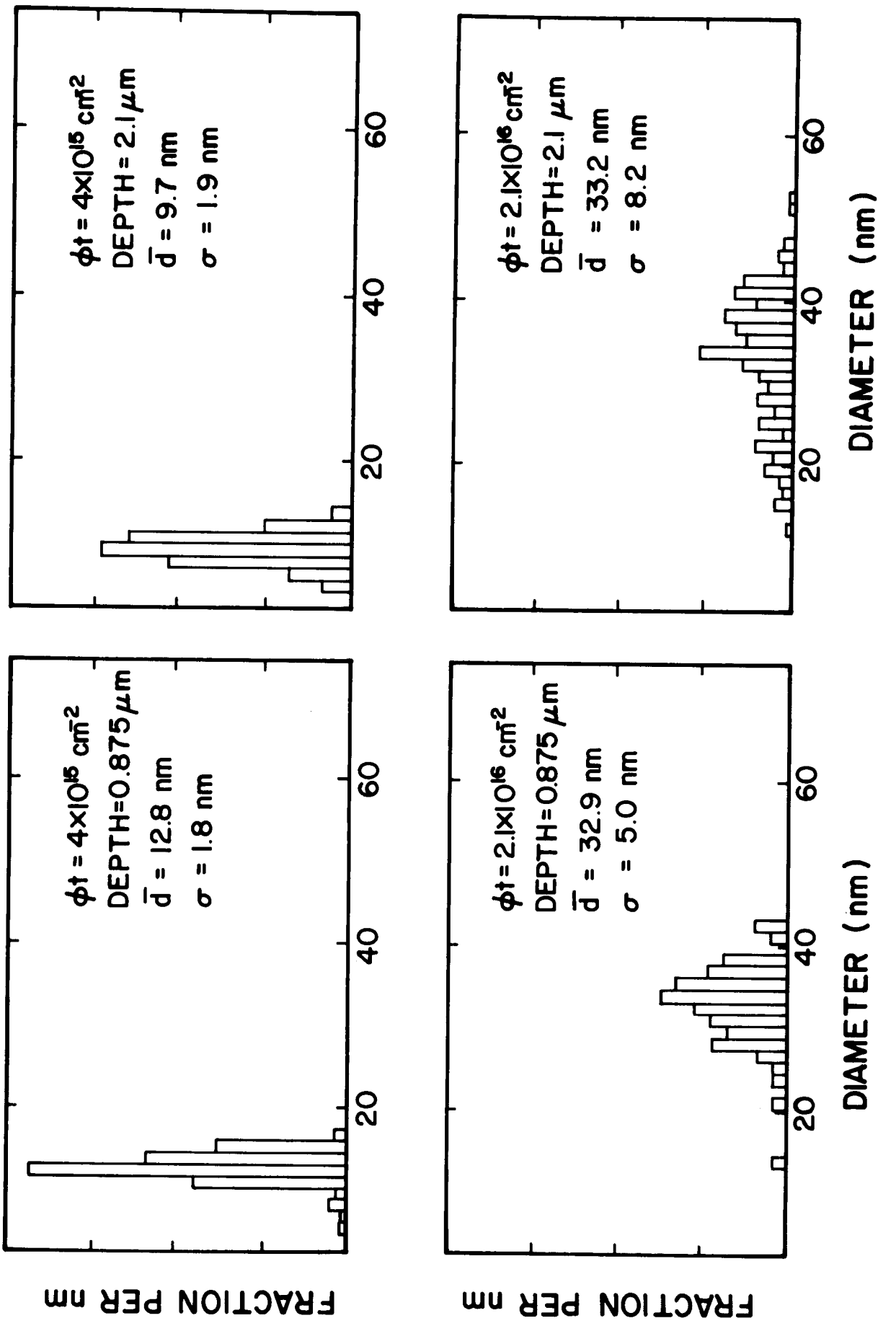

Figure 4. Void size distributions at two depths in nickel irradiated with aluminum ions to two fluence levels.

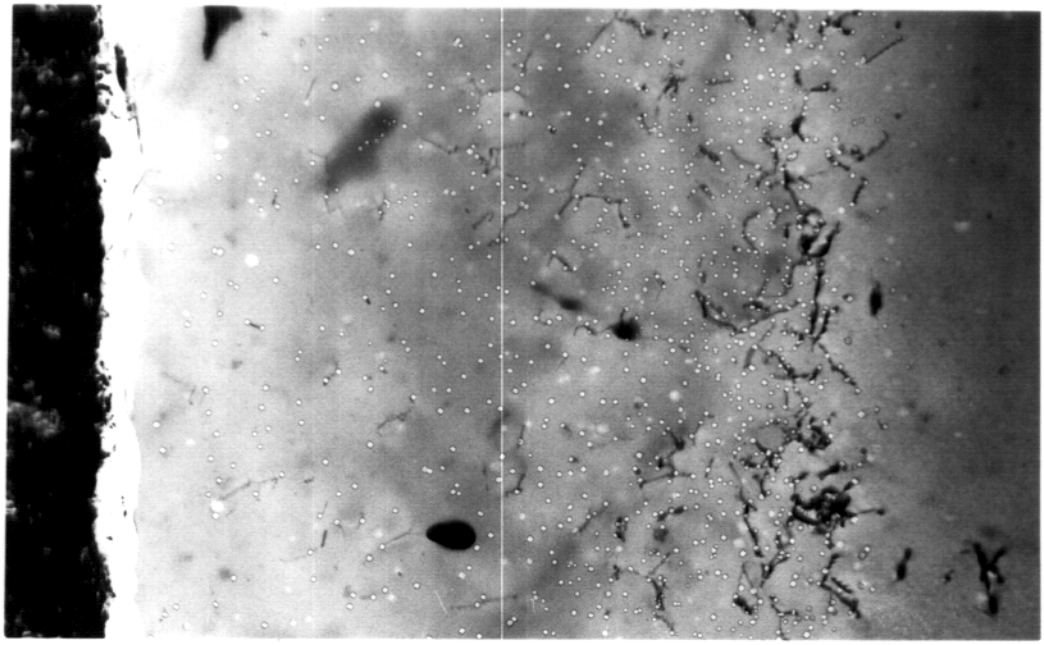

a) $1.5 \times 10^{16} cm^{-2}$

b) $9.2 \times 10^{16} cm^{-2}$

0.5 μm

Figure 5. Nickel irradiated at 525°C (798°K) with 5 MeV carbon ions to two fluence levels.

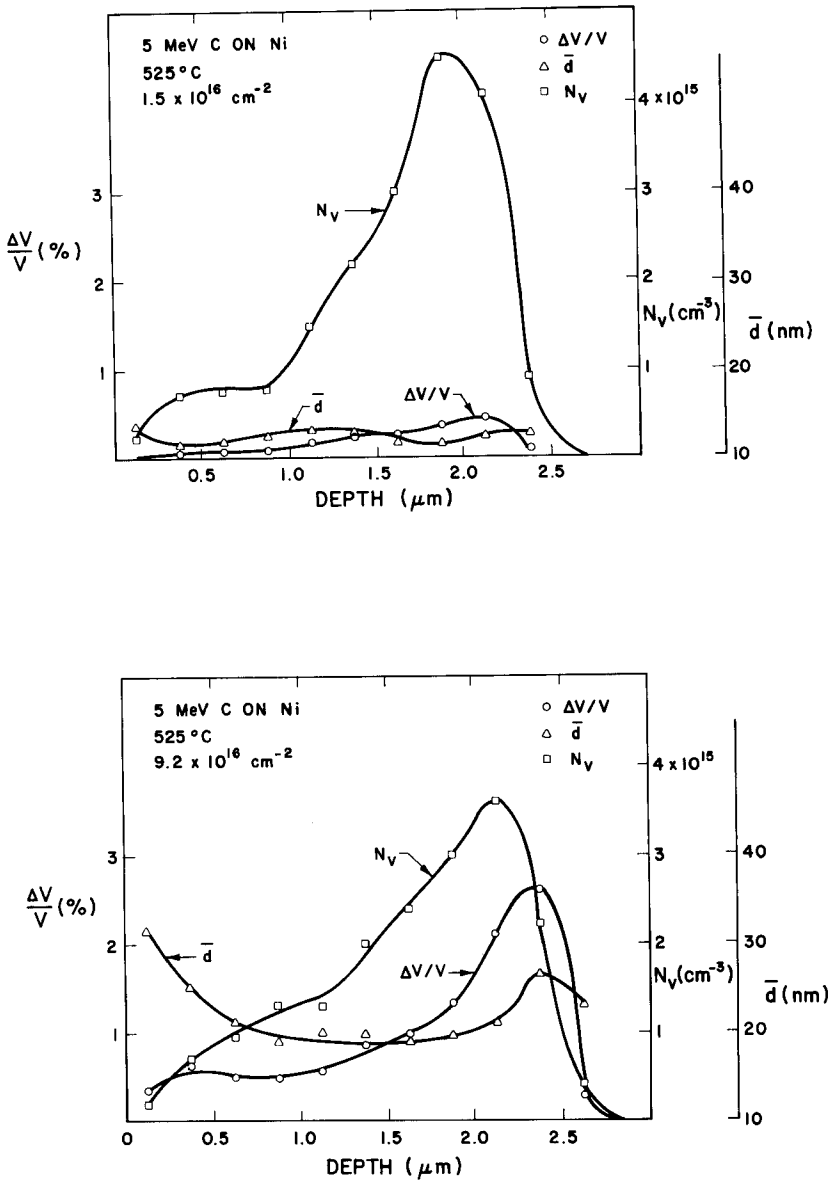

Figure 6. Average void diameter, void density, and void volume fraction as a function of depth in nickel irradiated with carbon ions to two fluence levels.

and the end-of-range region where it is larger than average. The peak void swelling in the carbon irradiated samples occurred at 2.4 μm with a value of 2.6%. The theoretical damage peak of 12 dpa occurs at a depth of 2.0 μm.

C. Dislocation Structure Development

The dislocation structure observed after irradiation with carbon ions is shown in figure 7a. The structure consists mainly of network dislocations with a few scattered loops. The total dislocation density ranged from 10^{10} to 10^{11} cm/cm^3, and increased significantly in the end-of-range region.

The dislocation structure for the aluminum irradiated samples is shown for two fluence levels in figures 7b and 7c. Here, at the low fluence, the dislocation structure consists of a dense network of dislocations interwoven among the high density of voids. This structure contains very few loops and is confined to the end-of-range region. At the highest fluence, the dislocation density has been reduced somewhat while at the same time extending to the near surface region.

D. Comparison to Self-Ion Irradiations of Identical Specimens

The carbon and aluminum irradiations were designed such that a relatively direct comparison could be made with a self-ion irradiated specimen. In figure 8 such a comparison is shown where the ion fluences are such that the peak damage values vary from ~15 dpa for the nickel ion irradiated specimen to ~10 dpa for the aluminum ion irradiated specimen. The void data obtained from the self-ion irradiated specimen is shown in figure 8. The nickel ion sample was irradiated at a higher dose rate, however, with a nickel ion flux of 1.5×10^{12} ions/cm^2·s (1.6×10^{-3} dpa/s at the peak compared to 5×10^{-4} dpa/s for the carbon and aluminum irradiated specimens).

There were several differences in the void microstructure between these specimens. In the near surface region, the self-ion irradiated specimen had a much larger void size in the surface region than either the aluminum or carbon irradiated specimens. This increase in void diameter is similar

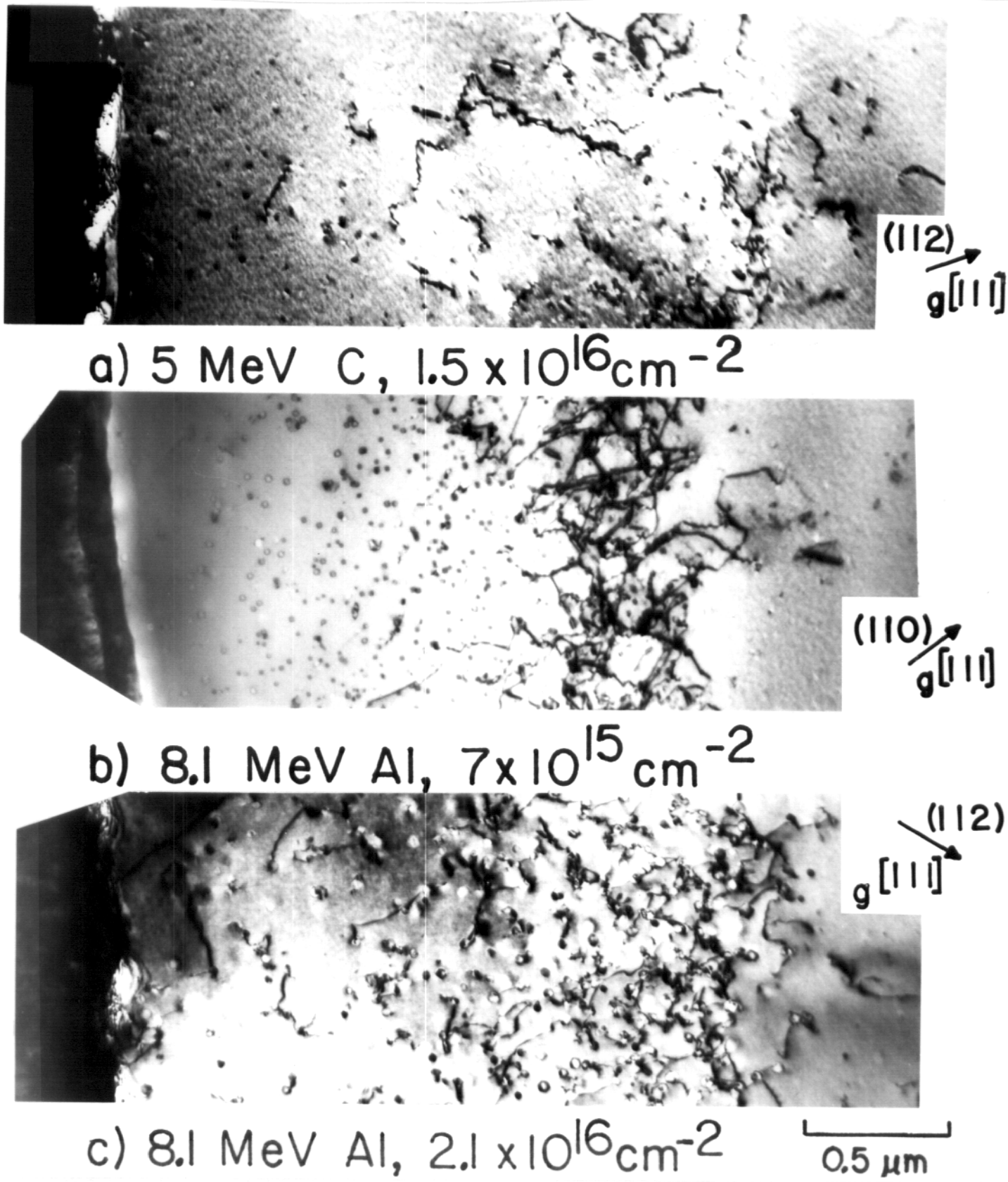

Figure 7. Dislocation structure development in ion irradiated nickel

a) after irradiation with carbon ions to a fluence of 1.5 x 10^{16} ions/cm^2;

b) after irradiation with aluminum ion to a fluence of 7 x 10^{15} ions/cm^2;

c) after irradiation with aluminum ions to a fluence of 2.1 x 10^{16} ions/cm^2.

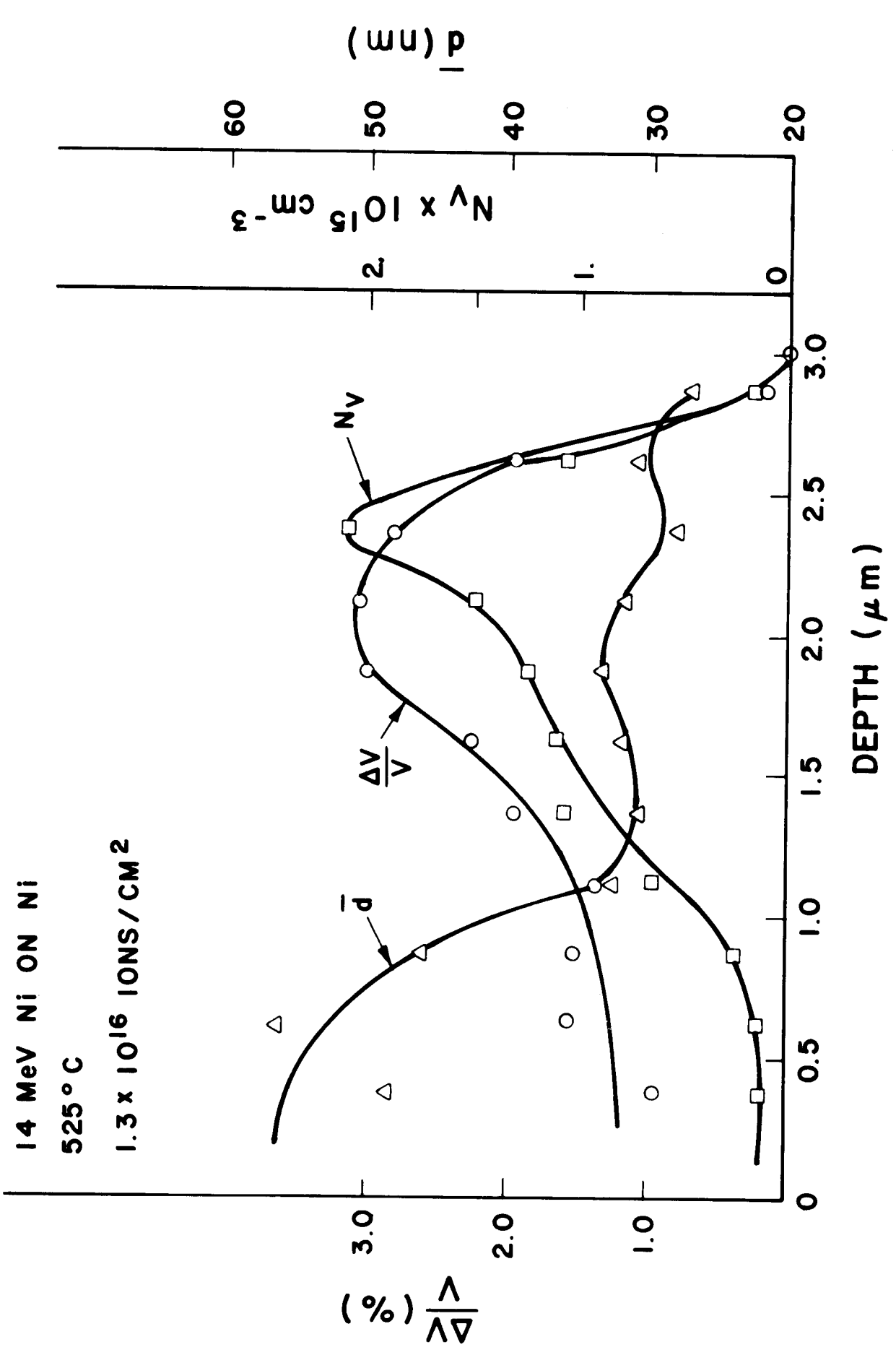

Figure 8. Average void diameter, void density, and void volume fraction as a function of depth is nickel irradiated with 14 MeV nickel ions at 525°C (798°K) to a fluence level of 1.3×10^{16} ions/cm^2.

to the increase seen next to grain boundaries in these specimens. The self-ion irradiated specimen showed a reduction in the void size in the end-of-range region which was not seen with the other ions. This reduction corresponds to the peak in the void density curve. After aluminum irradiation, there is little variation in the void density and this reduction in void size is not seen. The carbon ion irradiated sample fails to show a drop in void size with increasing void density, but does show an increase at the far end-of-range region.

All specimens contained voids at depths greater than the range of the damage curve. This is shown in figure 9, where the arrows on the micrographs indicate the predicted maximum ion range. The nickel ion irradiated sample showed a rather sharp void density cutoff with very few voids found beyond this range. Both the carbon and the aluminum irradiated samples failed to show this sharp cutoff, with a few scattered voids as much as 200-300 nm beyond the general void containing area.

IV. Discussion

A. Effects Due to Disparate Incident Ions

There are two basic differences between irradiations with different ions that could be expected to affect the final damage state of the material. The first is the change in chemical composition by implantation while the second is the change in cascade structure. These will be discussed in turn.

1. Excess Interstitials and Impurity Effects

An important difference between irradiations performed with different ions is the end-of-range effects due to the incident ion coming to rest in the materials. In both the aluminum and nickel ion irradiated samples, the incident ion behaves like a lattice atom and hence will represent an extra interstitial produced in these regions. Under low swelling rate conditions, (i.e., when defect loss by recombination or to unbiased sinks dominates) this small fraction of excess interstitials could significantly reduce the void swelling rate in the end-of-range region.[18] This effect is not believed

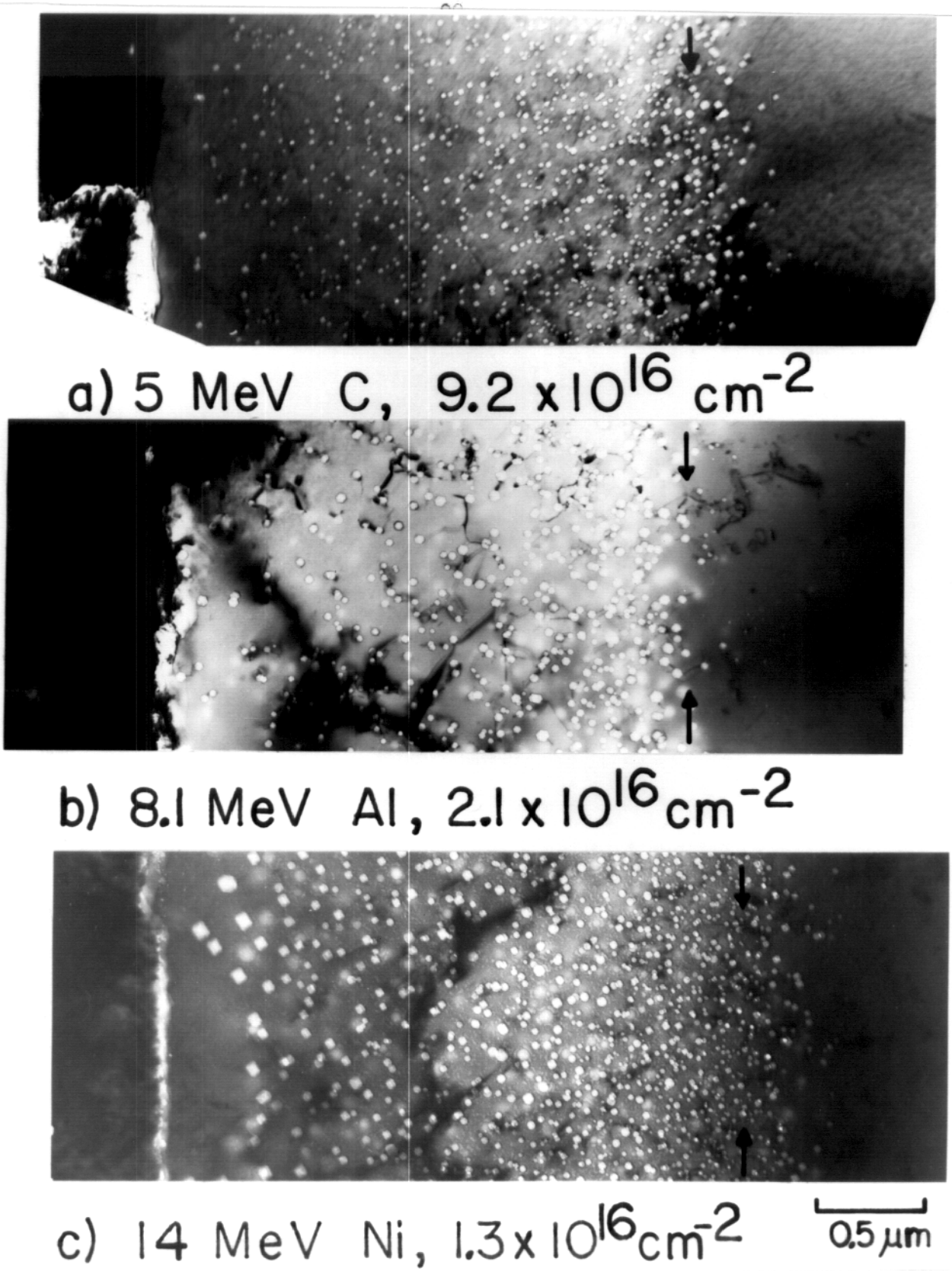

Figure 9. A comparison of nickel specimens irradiated at 525°C (798°K) with three different ions to fluence levels giving similar peak damage levels. The arrows near the right-hand-side of each micrograph indicate the predicted maximum ion range for the appropriate incident ion.

to be important for the high swelling rates observed in this study. In the case of aluminum or carbon irradiations, the incident ion represents an impurity which gradually increases in concentration as the irradiation proceeds. Since impurities often affect swelling behavior quite strongly, the end-of-range region of ion irradiated samples may be suspect. In this study, no major differences in void microstructure were observed in the end-of-range region of any of the specimens. The relatively small increase in void size at the end-of-range in the carbon sample may be due to an impurity effect such as a lowering of the surface energy.

Previous studies of nickel containing carbon[13] and nickel containing aluminum[14] before irradiation showed significant decreases in swelling when compared to pure nickel specimens. The studies of carbon doped nickel of Sorenson and Chen[13] found that a carbon level of 0.3 atomic percent would completely suppress void formation. In the high dose sample of this study, carbon was injected to a level of ≈0.4 atomic percent (assuming the carbon distributes itself uniformly throughout the damage region). In the previous studies, the impurity was present in significant amounts at the start of the irradiation and hence could play a significant role in the void and loop nucleation process. When the impurity is being introduced by the irradiating beam, it is still at very low concentration levels early in the irradiation sequence and hence cannot significantly alter the nucleation process in materials that nucleate voids as rapidly as the material used in this study. If an irradiation were to be continued to much higher fluence levels, it is possible that the effects of implanted impurities on the void growth rate would become evident. The major observation of this study was that the time history of the irradiation-impurity level is important in determining what effects, if any, will be seen.

This effect is important in considering such studies as simultaneous gas implantation with ion bombardment and in considering what effects transmutation reaction products might have on materials subject to neutron irradiation.

2. Cascade Effects

The second effect examined in this study is the different displacement cascade structures produced by ions of different mass. Previous studies on irradiated stainless steel[19,20] have found protons to be over ten times more effective in producing swelling than an equivalent dpa irradiation using nickel ions. This difference was believed due to the lower mass of the proton. The differential scattering cross-sections for the three different ions at two different depths are shown in figure 10. It can be seen that the primary knock-on (PKA) cross section, and hence the number of defects produced by a single incident ion, decreases with decreasing ion mass. With increasing depth, the cross-section for producing low energy PKA's will increase while the maximum energy that can be transferred is decreasing. One would expect the smaller displacement cascade of the light ions to allow less in-cascade recombination and hence release a larger fraction of the radiation produced defects to diffuse into the matrix. The results presented here, however, show that within a factor of two, there are no significant differences in the void microstructure that can be attributed to the different cascade structures.

B. Range Measurements

Both the carbon ion and aluminum ion irradiated specimens of this study contained a significant number of voids at depths ≈15% beyond the end-of-range given by the theoretical treatment of Brice.[11] In both cases, the peak of the swelling curve was also ~10% beyond the predicted peak of the damage curve. These results are consistent with previously reported results using nickel[5,6,8] and copper ions[6] incident on nickel, with the deviations from the predicted nickel and copper ion curves being somewhat larger. Narayan, et al.,[8] attribute this deviation in range to an underestimate of the

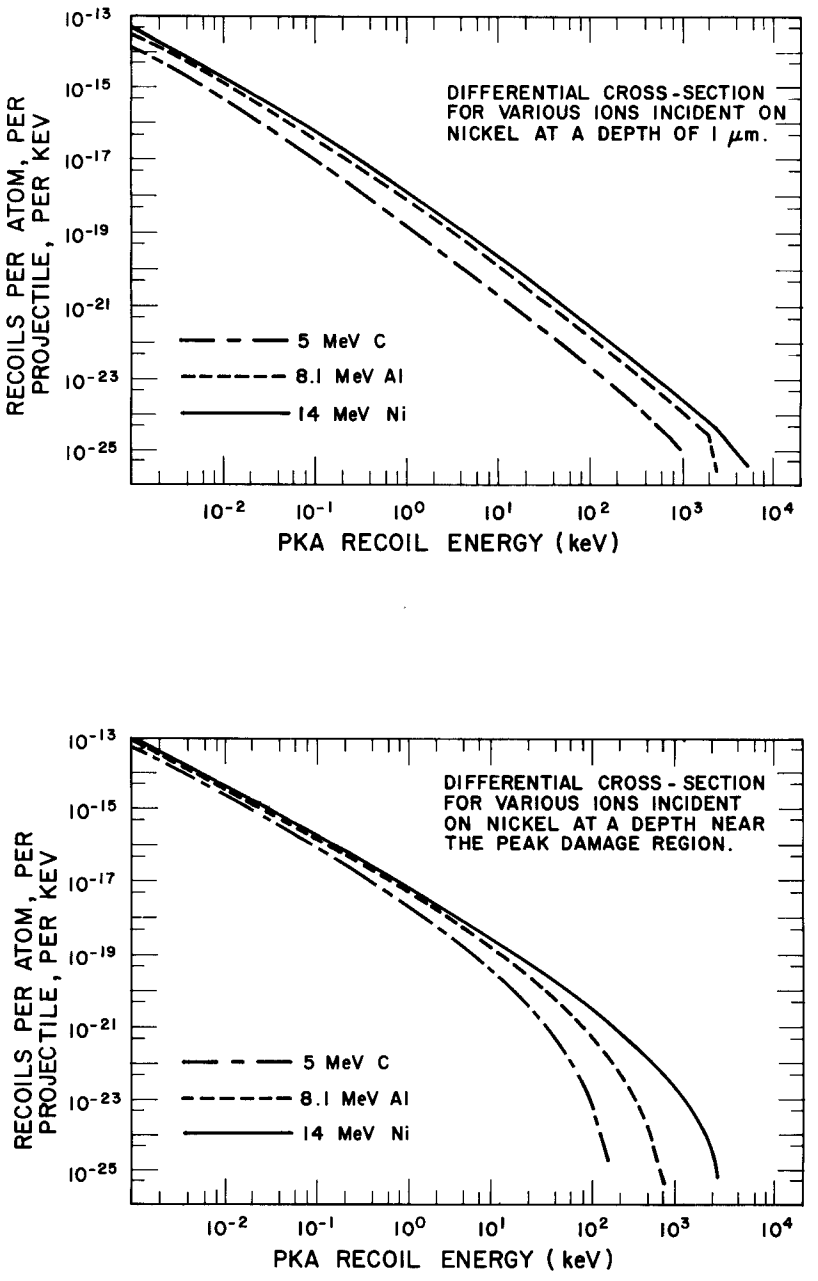

Figure 10. The primary recoil energy spectra for the three ions incident on nickel. The top curve corresponds to a depth of 1 μm, and the bottom curve a depth corresponding to the peak of the damage curve.

electronic energy loss by the incident ion. This seems to be a reasonable explanation, even though such mechanisms as vacancy diffusion down the steep concentration gradient at the end-of-range could allow void growth in an damage free region.

C. Void Density

Under the aluminum ion irradiation, the void number density was observed to be a maximum at the lowest ion fluence, and then to drop with increasing fluence. Similiar behavior has been observed previously in nickel[21,22] and is not believed to be due to void impingement, but rather due to local changes in the microstructure.[22] In the material prepared for this study, voids did nucleate quite easily. This apparently leads to such a high void density that continuing the irradiation beyond that necessary to nucleate the voids causes a subsequent change in the microstructure which allows some of the voids to continue to grow, with the rest shrinking and disappearing. Possible causes for this behavior include a) an increase in the void critical size, b) the dislocations connecting the voids leading to enhanced void coarsening, and c) the lower vacancy concentration due to the increasing sink density.[23] The data from this study was not sufficient to determine which mechanism was valid.

Conclusions

The depth dependent void microstructure in nickel irradiated at 525°C with carbon and aluminum ions was measured and the following conclusions were drawn:

1. Any end-of-range effects due to the irradiating ions stopping in the material are minimal. This demonstrates the importance of the impurity-irradiation time history, with impurities present in significant amounts at the start of the irradiation being much more important than impurities added during the irradiation.

2. Voids were observed at depths ≈15% beyond the predicted damage curve, indicating that either the theoretical energy loss models are in error or that vacancies are transported over large distances from their point of origin.

3. The void density was a maximum at the lowest carbon and aluminum ion fluences, and dropped with increasing ion fluence. This indicates that the critical void size for growth is increasing with the growing void and dislocation microstructure.

4. The differences in the PKA spectra from carbon, aluminum, and nickel irradiations does not appear to have any major effect on the nucleation and growth of voids.

Acknowledgements

This research was sponsored by the Department of Energy, Office of Fusion Energy, under contract number ET-78-S-02-4640. The authors are grateful to the University of Wisconsin Nuclear Physics Group for the use of the tandem accelerator and its facilities.

References

1. W. G. Johnston, J. H. Rosolowski, and A. M. Turkalo, Journal of Nuclear Materials 62, 1976, pp. 167-180.

2. C. W. Chen, A. Mastenbroek, J. D. Elen, Radiation Effects 16, 1972, pp. 127-132.

3. S. Diamond, I. M. Baron, M. L. Blieberg, R. Bajaj, and R. W. Chichering, Proceedings of International Conference on Radiation Effects and Tritium Technology for Fusion Reactors, Gatlinburg, Tenn., Oct. 1975, Vol. I, pp. 207-229.

4. A. F. Rowcliffe, S. Diamond, M. L. Bleiberg, J. Spitznagel , and J. Choyke, Properties of Reactor Structural Alloys After Neutron or Particle Irradiation, ASTM STP 570, American Society for Testing and Materials, 1975, pp. 565-583.

5. J. B. Whitley, P. Wilkes, and G. L. Kulcinski, UWFDM-159, University of Wisconsin, Madison, Wisconsin, 1976.

6. J. B. Whitley, G. L. Kulcinski, P. Wilkes and H. V. Smith, Jr., submitted to Journal of Nuclear Materials, (1978).

7. R. A. Spurling and C. G. Rhodes, Journal of Nuclear Materials 44, 1972, pp. 341-344.

8. J. Narayan and O. S. Oen, Journal of Nuclear Materials 66, 1977, pp. 158-162.

9. J. Narayan, O. S. Oen, and T. S. Noggle, Journal of Nuclear Materials 71, 1977, pp. 160-170.

10. J. B. Whitley, P. Wilkes, G. L. Kulcinski, Transactions of The American Nuclear Society, Vol. 23, 1976, pp. 136-137.

11. D. K. Brice, SAND75-0622, Sandia Laboratories, Albuquerque, New Mexico, July 1977.

12. I. Manning and G. P. Mueller, Computer Physics Communication 7, 1974, pp. 85-94.

13. S. M. Sorenson, Jr., and C. W. Chen, Proceedings of International Conference on Fundamental Aspects of Radiation Damage in Metals, Gatlinburg, Tenn., Oct. 1975, CONF 751006, pp. 1213-1220.

14. F. A. Smidt, Jr., and J. A. Sprague, Naval Research Laboratory Memorandum Report 2998, 1975, pp. 39-51.

15. R. G. Lott and H. V. Smith, Jr., Symposium on Experimental Methods for Charged Particle Irradiation, Gatlinburg, Tenn., CONF 750947, Sept. 1975, pp. 82-98.

16. H. V. Smith, Jr., and R. G. Lott, Nuclear Instruments and Methods 143, 1977, pp. 125-132.

17. H. V. Smith, Jr. I.E.E.E. Transactions on Nuclear Science, NS-23, 1976, p. 1118, to be published.

18. A. D. Brailsford and L. K. Mansur, Journal of Nuclear Materials 71, 1977, pp. 110-116.

19. G. L. Kulcinski, Applications of Ion Beams to Metals, Plenum Corporation, N.Y., 1974, pp. 613-637.

20. D. W. Keefer and A. G. Pard, Journal of Nuclear Materials, 47, 1973, p. 97.

21. J. A. Sprague, J. E. Westmoreland, F. A. Smidt, Jr., and P. R. Malmberg, Consultant Symposium on The Physics of Irradiation Produced Voids, Harwell, Oxfordshire, U. K., 1974, pp. 263-267.

22. T. D. Ryan, Ph.D. Thesis, University of Michigan, 1975. (Available from University Microfilms, Ann Arbor, Michigan, U.S.A.).

23. N. Ghoniem and G. L. Kulcinski, Journal of Nuclear Materials, 69,70, 1978. pp. 816-820.